Supplementary Information

A facile wet-chemistry approach to engineer Au-based SERS substrate and enhance sensitivity down to ppb-level detection

Chien-Wei Lee,[a] Zi Chun Chia,[a] Yi-Ting Hsieh,[b] Hsiao-Chieh Tsai,[b] Yenpo Tai,[c] Teng-To Yu[c] and Chih-Chia Huang*[a]

[a]Department of Photonics, Center for Micro/Nano Science and Technology, Center of Applied Nanomedicine, National Cheng Kung University, Tainan 70101, Taiwan.
[b]Department of Chemistry, Soochow University, Taipei 11102, Taiwan
[c]Department of Resources Engineering, National Cheng Kung University, Tainan 70101, Taiwan.

E-mail: c2huang@mail.ncku.edu.tw; huang.chihchia@gmail.com

Experimental

Laser spot size: The diameter of laser spot can be estimated by the following equation (1):

$$\mathbf{d} \approx \frac{\mathbf{1.22}\ \lambda}{\mathbf{n}\ \sin\theta} = \frac{\mathbf{1.22}\ \lambda}{\mathbf{NA}} \tag{1}$$

where λ is the laser wavelength and NA is the numerical aperture.

In our study, λ = 785 nm, NA = 0.5, so d ≈ 1.915 μm, giving a laser spot size of 2.88 μm^2.

Number of MB molecules excited for normal Raman (N_{Raman}):

For paper substrate without Au NPs, initial bulk MB = 10 mM × 6 μL = 6 × 10^{-8} mole of MB molecules. We assumed that these MB molecules are homogeneous distribution into a paper (28.274 mm^2), possessing the density of MB molecules as ≈ 2.122 × 10^{-15} mole per μm^2. Concerning the laser spot size at 2.88 μm^2, the laser light area would cover 6.11 × 10^{-15} mole of MB molecules by measuring 2.88 μm^2 × 2.122 × 10^{-15} mole/μm^2. Finally, this N_{Raman} ≈ 3.68 × 10^9 MB molecules is irradiated by the laser during normal Raman acquisition on the paper substrate. A following equation (2) could be utilized to determine the N_{Raman} of the different analytes.

$$\mathbf{N_{Raman}} = \frac{\mathbf{C_{Normal} \times d \times N_A}}{\mathbf{S}} \tag{2}$$

where C_{Normal} is the concentration of MB when used in the pure paper, d is a laser spot size, N_A is the Avogadro's number, and S is surface area of a paper.

Number of MB molecules excited for SERS with Au NPs (N_{SERS}):

Due to the Au NPs in the inner layer of HH substrate was not possible to determined according to the SEM image of a surface-related analysis method, an

accurate measurement of the molecule number on the Au nanoparticles is pretty difficult. Thus, we utilized an analytical enhancement factor (AEF) method to estimate the SERS enhancement efficiency.

For SERS measurement, 6 µL of MB (100 nM) was equal to 6×10^{-13} mole which was added into the HH substrate. Again, it has assumed the homogeneous distribution of MB molecules into a paper (28.274 mm^2). The density of MB molecules is estimated to be $\approx 2.122 \times 10^{-20}$ mole per µm^2, and the laser irradiated area (2.88 µm^2) involved 6.11×10^{-20} mole into a HH substrate. This $N_{SERS} \approx 3.68 \times 10^4$ MB molecules was determined within the laser light during Raman acquisition on the HH substrate. A following equation (3) could be utilized to determine the N_{SERS} of the different analytes.

$$N_{SERS} = \frac{C_{SERS} \times d \times N_A}{S} \qquad (3)$$

where C_{SERS} is the concentration of MB when used in the HH substrate, d is a laser spot size, N_A is the Avogadro's number, and S is surface area of a HH substrate.

Calculated analytical enhancement factor (AEF) with MB molecules:

The value of AEF is obtained experimentally using following equation (4):

$$AEF = \frac{I_{SERS}}{I_{Normal}} \frac{C_{Normal}}{C_{SERS}} \qquad (4)$$

where $I_{SERS} \approx 1203.88$ count and $I_{Normal} \approx 1635.81$ count are the Raman intensity signals at 1620 cm^{-1} of MB that collected using the HH substrate and paper substrate, respectively (Fig. S7). C_{SERS} and C_{Normal} are the concentration of MB molecules within laser from the measurements of the HH substrate and paper substrate, respectively. So, here we can get AEF of HH substrate $\approx 1.36 \times 10^5$.

Table S1 Comparison of the experimental methods and analytical enhancement factor (AEF) values with other studies.

SERS substrate	SERS preparation method	AEF	Reference
HH-Au SERS substrate	Secondary growth reaction of crude SERS substrate via a wet-chemistry approach	1.36×10^5 (MB; 785 nm; 5 mW; 10 s) 7.36×10^5 (MG; 633 nm; 2.5 mW; 10 s)	This work
Ag NPs substrates (Pen-on-Paper)	Writing by using a nanoparticle ink-filled pen.	2×10^5 (532 nm; 10 s) 1.5×10^5 (785 nm; 10 s)	1
Colloidal Au Au nanospheres	Directional assembly of Au NPs with cucurbit[n]uril	3×10^3 (MV; 633 nm; 20 s)	2
Au NPs growth on mesostructured silica film substrate	Repeatedly immersing chemicals and Au seeds into the mesostructured silica copolymer film.	5×10^1 (R6G; 633 nm; 20 s)	3
Star-shaped gold nanostructures	Aggregation of Au nanoparticles in HCl solution	5×10^6 (R6G; 633 nm; 20 s)	3
40-50 nm Au@citrate nanoparticles	Aggregation of Au@citrate nanoparticles in NaCl solution	11×10^5 (R6G; 633 nm; 20 s)	3
Au nanostars (AuNSts) on a glass substrate	Chemical deposition of the AuNSts onto the 3-	5.7×10^2 (CV; 532 nm; 13.5 mW; 1 s)	4

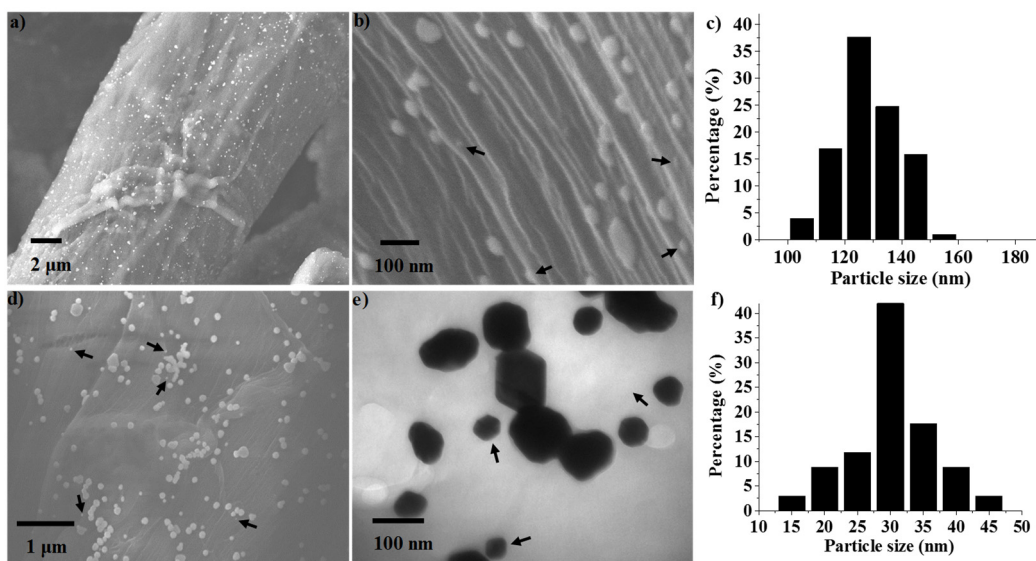|		aminopropyltriethoxysilane-functional glass surface			
Colloidal Au nanostars		Colloid-based seed-mediated growth process by using sodium citrate and HQ as both the reducing reagent and capping ligand	10^4	(4-mercapto benzoic acid and MG; 1064 nm; 373 mW; 5 s)	5

Fig. S1 a) Low-magnification SEM image (5000 x), b) high-magnification SEM image (100000 x), d) high-magnification SEM image (20000 x), and e) TEM image (200000 x) of Au@TNA NPs in the Au@TNA SERS substrate. The arrows indicate smaller particles, which are difficult to observe in the low-magnification SEM image. c) Percentage and average particle size of Au@TNA NPs in the Au@TNA SERS substrate according to the SEM images in a) and d). Over 100 nm was selected for those particle density measurements. f) Percentage and average particle size of the smaller pristine Au seeds in the TEM and SEM image (Fig. S1b,d,e) of the initial Au@TNA substrate. Below 100 nm was selected for those particle density measurements.
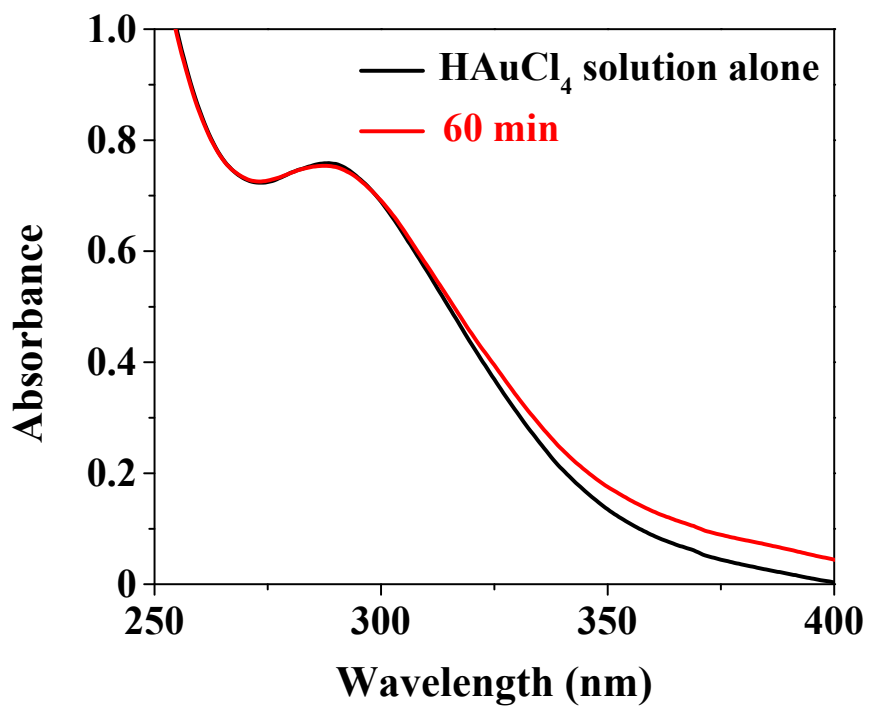
Fig. S2 UV-vis spectra for the absorption band[6] of HAuCl₄ before and after reacting with purified Au@TNA substrate.
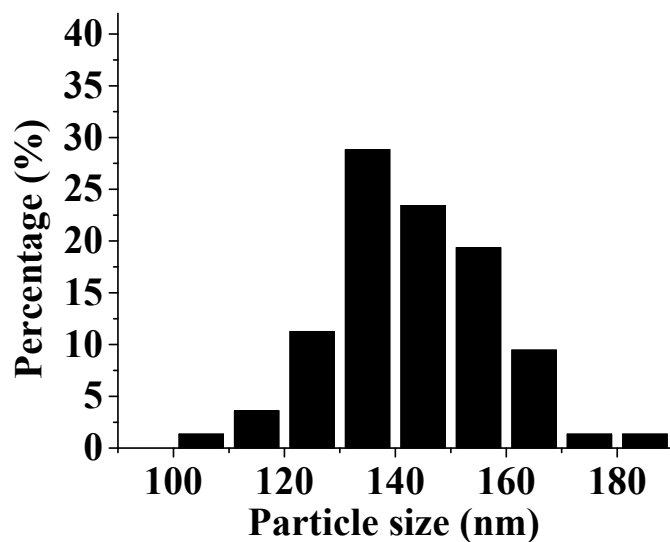
Fig. S3 Percentage and average particle size of the HH substrate.
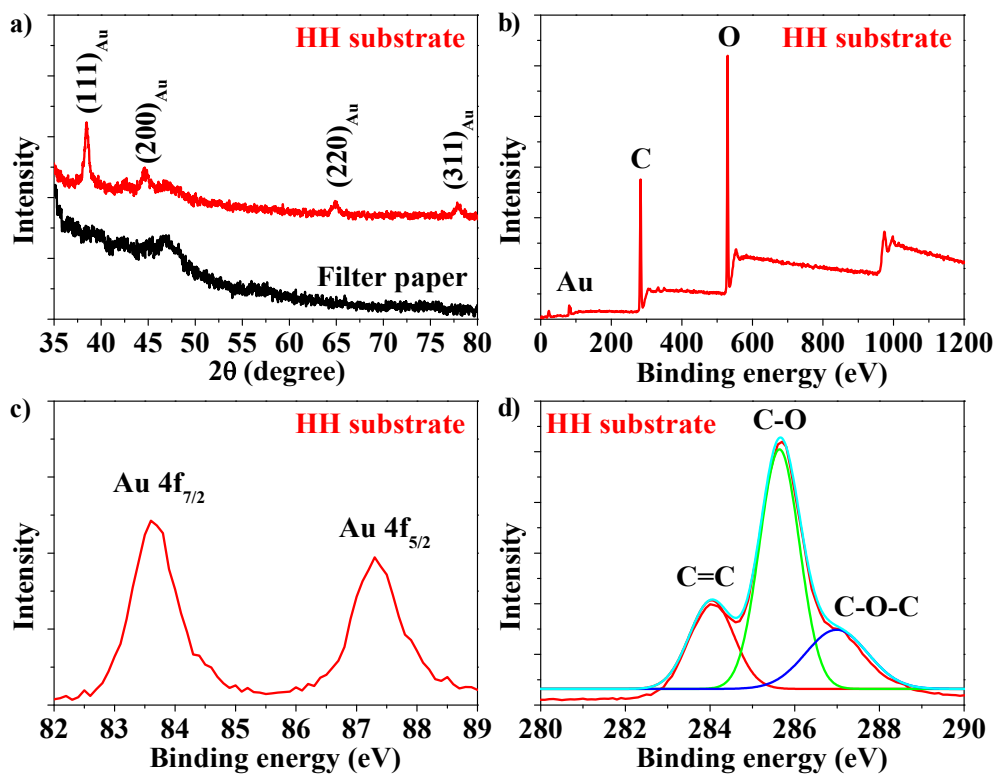
Fig. S4 a) XRD pattern and b) XPS analysis of the HH substrate. The high resolution c) Au4f peak and d) C1s peak in the XPS spectrum for the HH substrate.
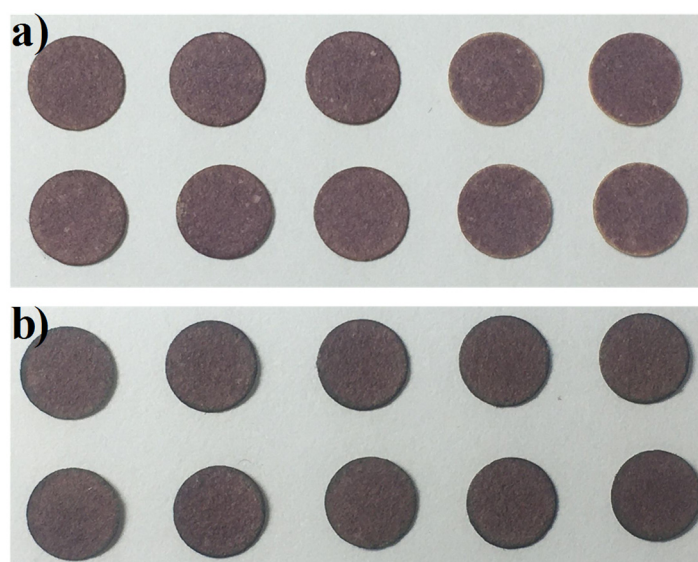

Fig. S5 Photograph of the a) purified Au@TNA SERS substrates and b) HH substrates. The HH substrates are prepared by a single postreaction process with ten purified Au@TNA SERS substrates.
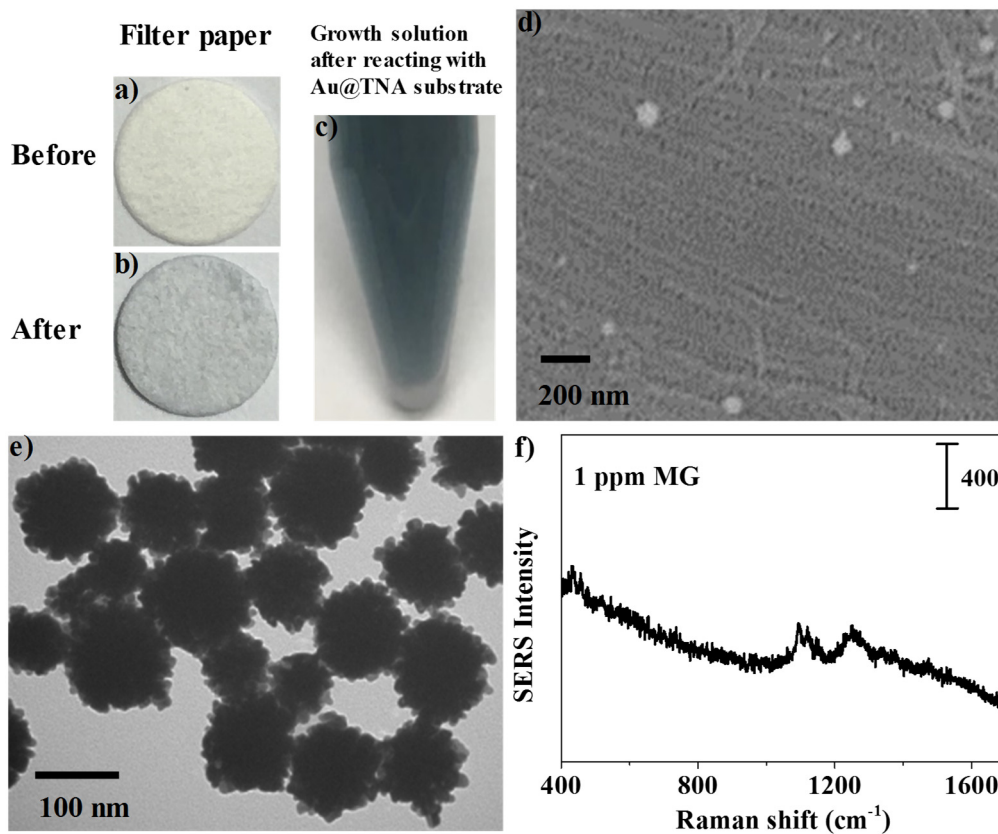
Fig. S6 Photographs of a) pure filter paper, b) the resulting product after reacting of pure filter paper with HAuCl₄ and HQ molecules, and c) the supernatant from the growth solution after reacting with Au@TNA substrate. d) SEM image of the product in Fig. S6b and e) TEM image of the colloidal product (103.6 ± 17.2 nm) in Fig. S6c. f) SERS spectrum of MG obtained with the product substrate shown in Fig. S6b.
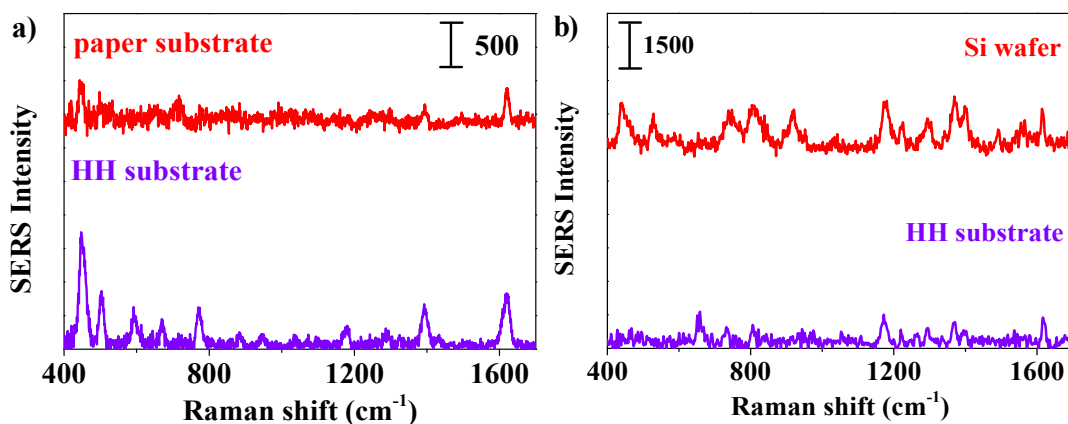
Fig. S7 SERS spectra of a) 10 mM MB on filter paper, 100 nM MB on the HH SERS substrates and b) 1000 ppm MG droplet on a Si wafer, 1 ppb MG with the HH SERS substrates.
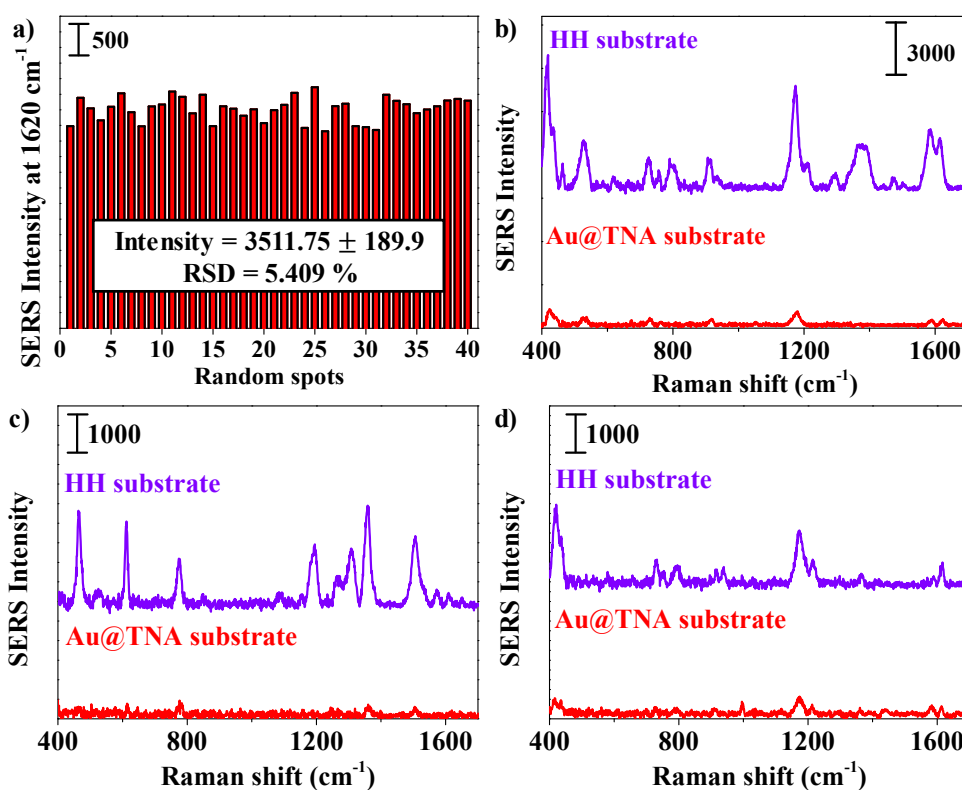
Fig. S8 SERS signal data for a) 40 different data points at 1620 cm^{-1} for 0.01 mM MB with the HH substrate. SERS spectra of b) 0.01 mM CV, c) 0.01 mM R6G, and d) 0.01 mM MG with the Au@TNA substrate and HH substrate.
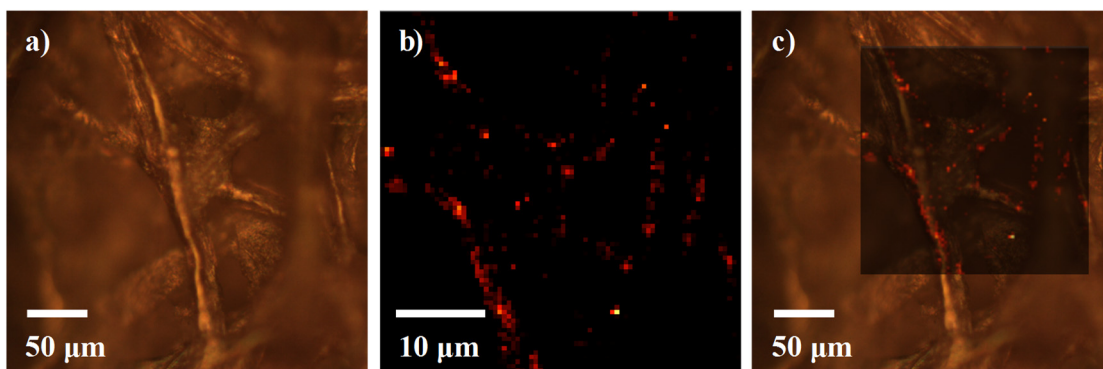
Fig. S9 a) Bright field image, b) SERS mapping signal, and merged results of a) and b) for 0.1 mM MBN on the HH substrate by using a confocal Raman scanning system.
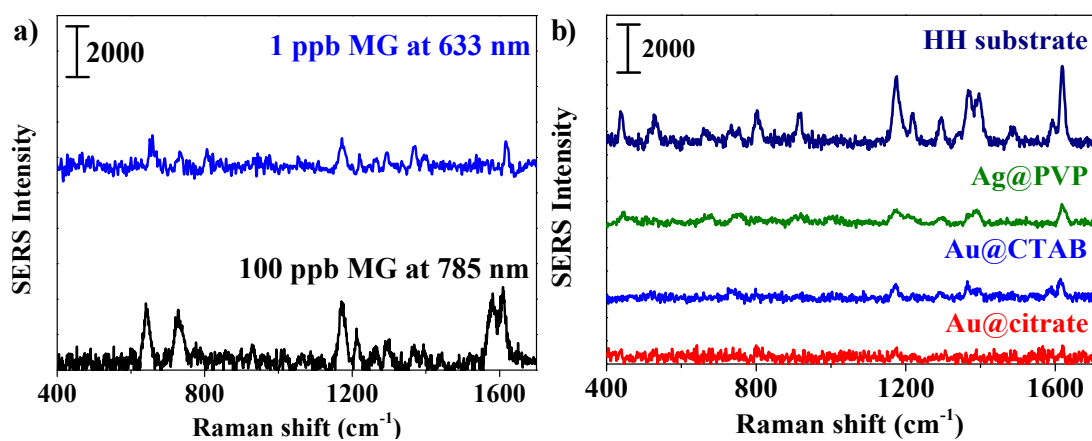
Fig. S10 SERS spectra of a) 1 ppb and 100 ppb MG on the HH substrate with 633 nm and 785 nm lasers. b) SERS detection of 100 ppb MG with the HH substrate, 13 nm Au@citrate NPs-SERS substrate, 150 nm Au@CTAB NPs-SERS substrate, and 80 nm Ag@PVP NPs-SERS substrate with the 633 nm laser.
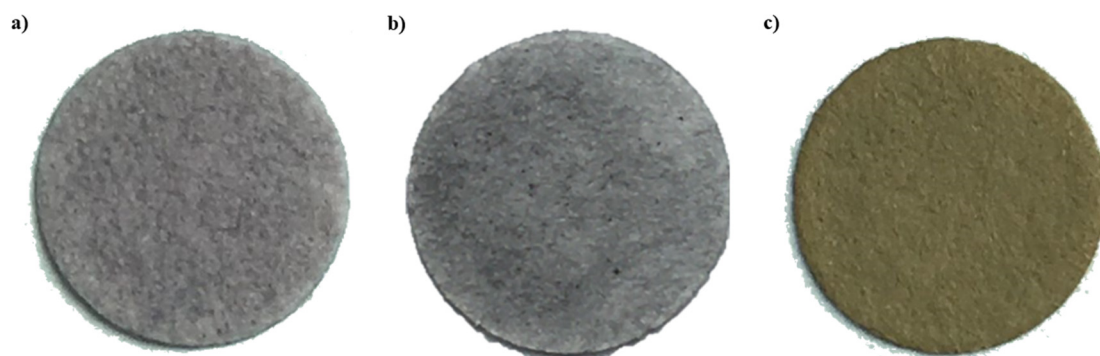
Fig. S11 Photograph images of a) 13 nm Au@citrate NPs-SERS substrate, b) 150 nm Au@CTAB NPs-SERS substrate, and c) Ag@PVP NPs-SERS substrate.
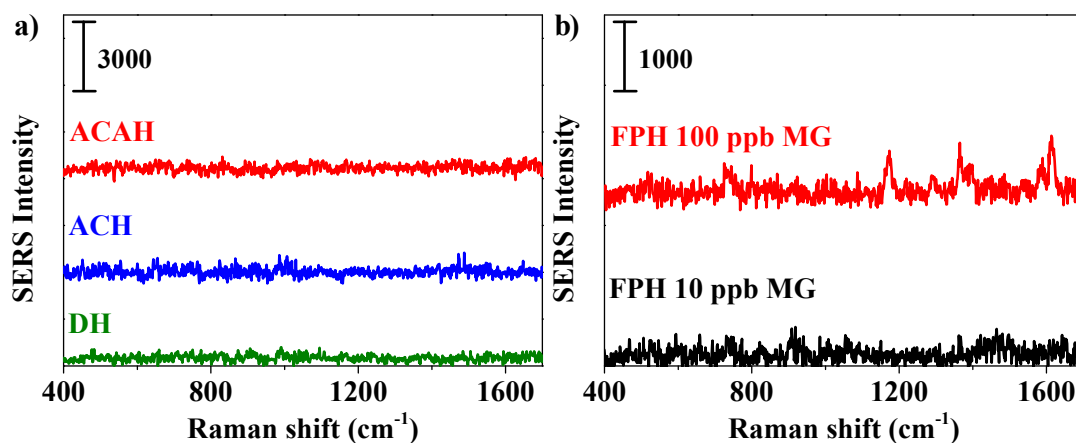

Fig. S12 SERS spectra of a) 100 ppb MG with the ACAH, ACH, DH-SERS substrate, and b) 100, 10 ppb MG with the FPH-SERS substrate with the 633 nm laser.
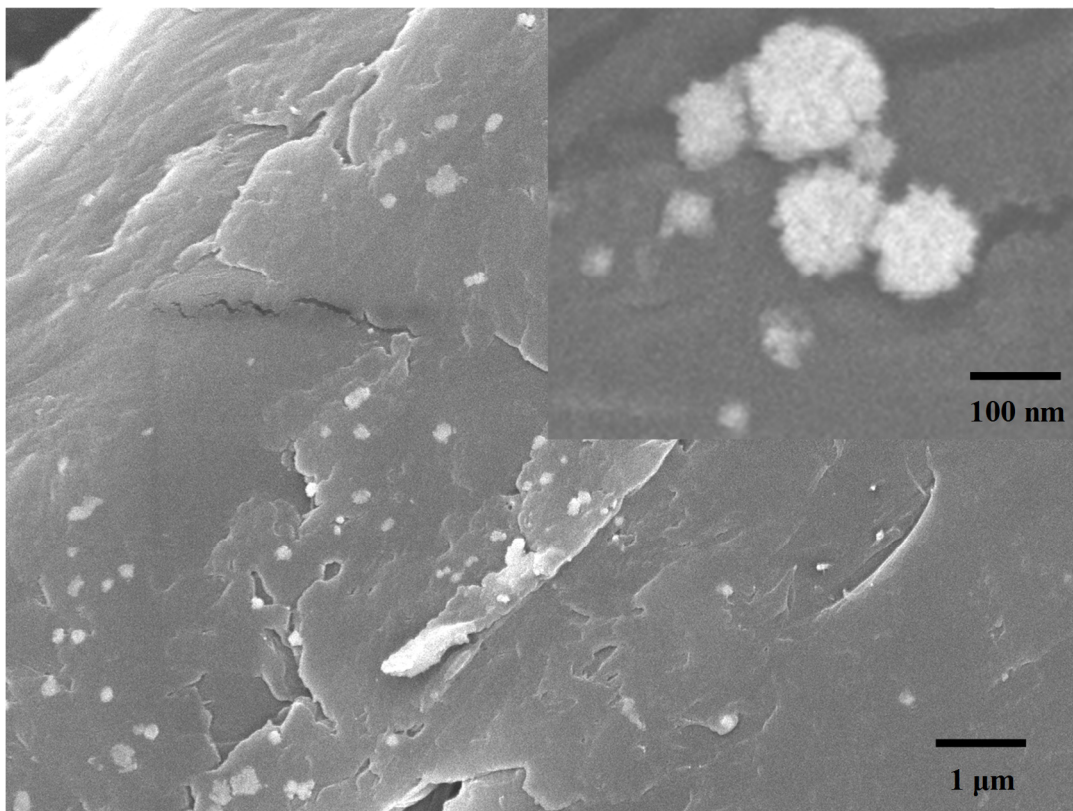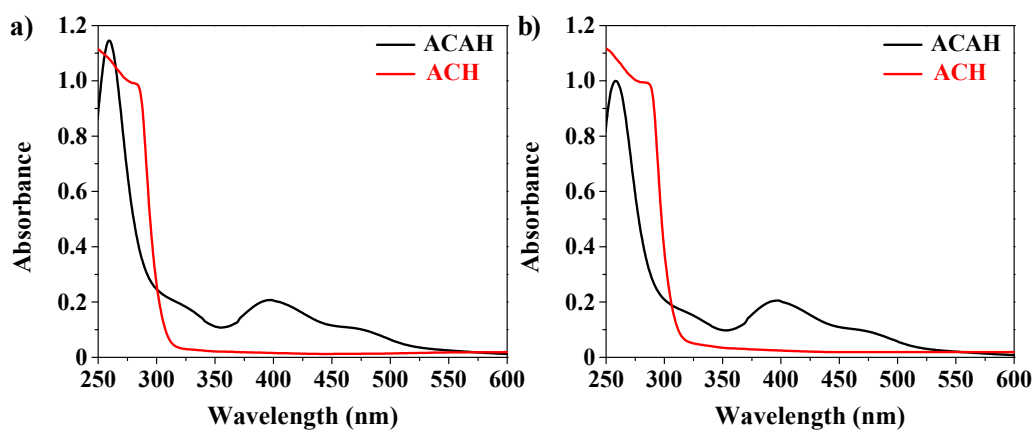
Fig. S13 SEM image of a peeled HH substrate.

Fig. S14 UV-vis spectra of AuCl$_2^-$/CTAB complex in the ACAH and ACH solutions a) before and b) after reacting with the Au@TNA substrates.
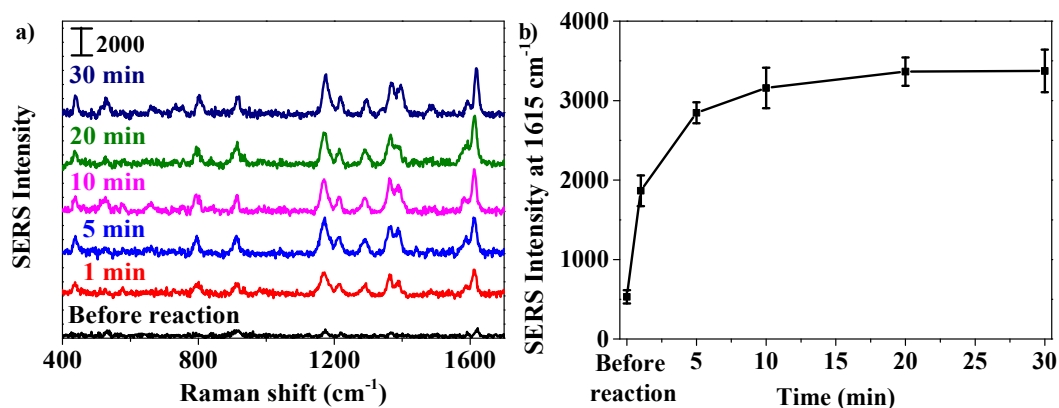
Fig. S15 a) SERS spectra and b) SERS intensity at 1615 cm^{-1} responsed to 100 ppb MG by using different HH substrates preared after reacting Au@TNA and HH-based solution at 1, 5, 10, 20, and 30 min. Data collected by using a 633 nm Raman system.
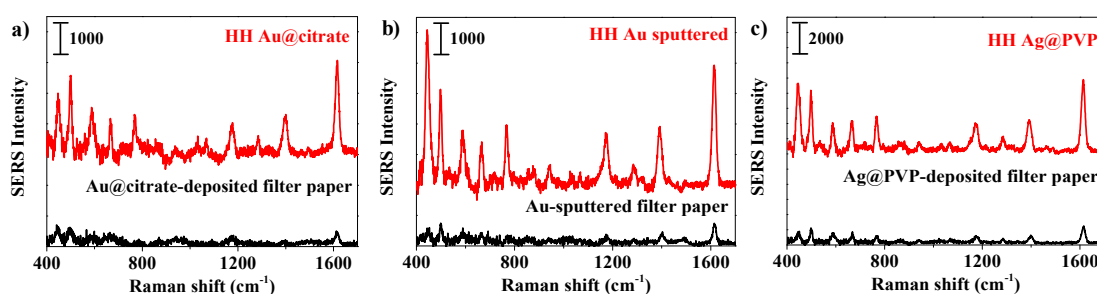

Fig. S16 SERS spectra of 0.1 mM MB on the different metal-adsorbed filter substrates (black curves) and HH-based SERS substrates (red curves) with a 785 nm Raman system. A sputtered Au substrate prepared by directly depositing gold nanocrystals onto a filter paper with a JFC-1100 fine coat ion sputter (U = 2.5 kV, I = 10 mA, and t = 3 min). Au@citrate NPs (~50 nm) and Ag@PVP NPs (~80 nm) are prepared according to the previous methods in the literature.[7,8]
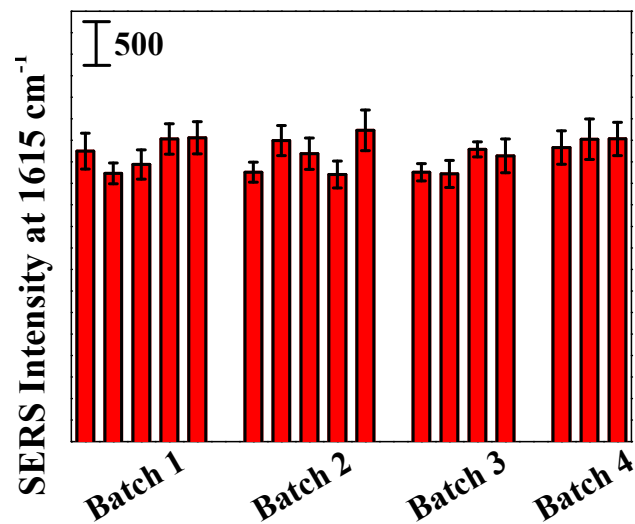
Fig. S17 Batch-to-batch SERS reproducibility (at 633 nm) of 100 ppb MG on the HH substrates. Data represent as mean with standard deviation (SD) of five independent measurements.
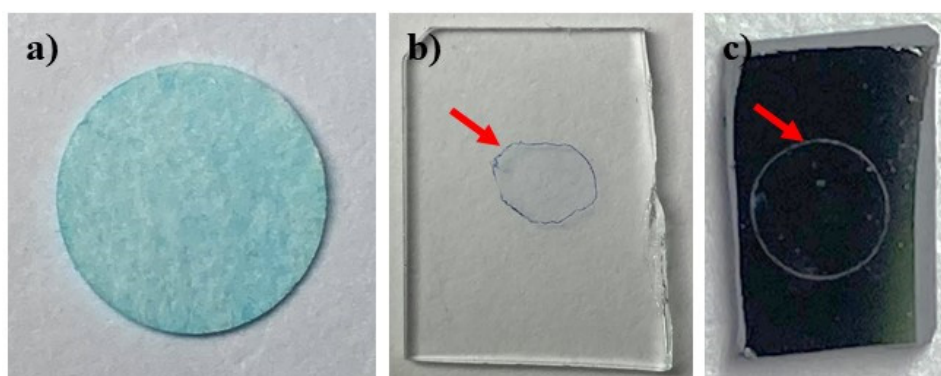

Fig. S18 Photographs of 10 μL MB droplet (0.01 mM MB) dried on the (a) filter paper, (b) glass substrate, and (c) silicon wafer. The red arrows indicate the coffee ring stains.
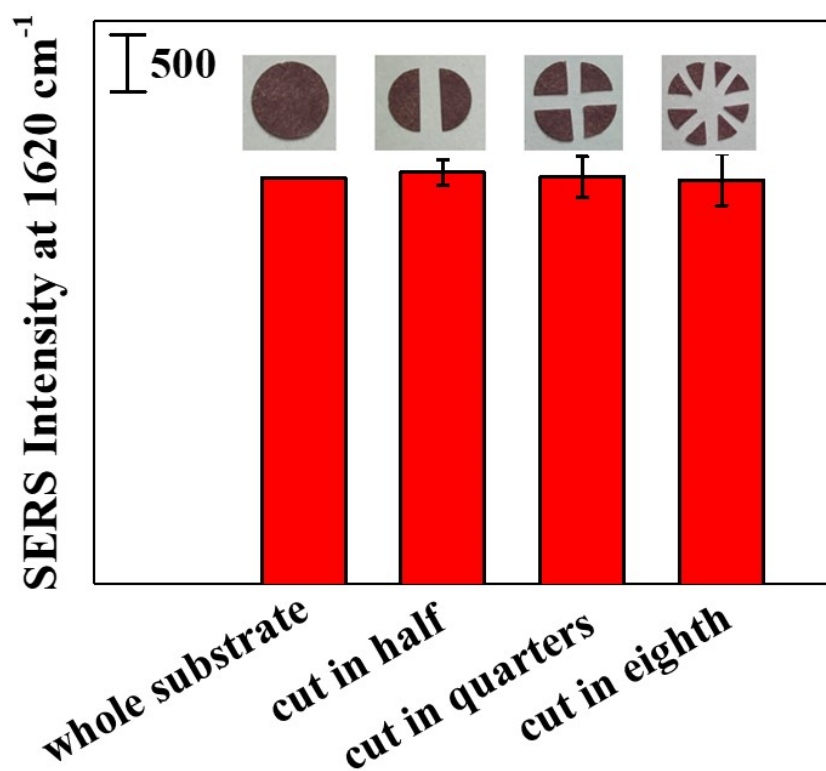
Fig. S19 The mean SERS signals recorded at 1620 cm^{-1} for 0.01 mM MB into the individual slides from the HH substrate in different proportion: whole, half, quarter, eighth HH substrtaes (from left to right).

Reference

1. L. Polavarapu, A. La Porta, S. M. Novikov, M. Coronado-Puchau and L. M. Liz-Marzán, *Small*, 2014, **10**, 3065−3071.

2. J. C. Fraire, V. N. Sueldo Ocello, L. G. Allende, A. V. Veglia and E. A. Coronado, *J. Phys. Chem. C*, 2015, **119**, 8876−8888.

3. E. Akanny, A. Bonhommé, L. Bois, S. Minot, S. Bourgeois, C. Bordes and F. Bessueille, *Chemistry Africa*, 2019, **2**, 309–320.

4. N. Schwenk, B. Mizaikoff, S. Cárdenas and Á. I. López-Lorente, *Analyst*, 2018, **143**, 5103–5111.

5. X. Meng, J. Dyer, Y. Huo and C. Jiang, *Langmuir*, 2020, **36**, 3558–3564.

6. A. Vogler and H. Kunkely, *Coord. Chem. Rev.*, 2001, **219–221**, 489–507.

7. N. G. Bastús, J. Comenge and V. Puntes, *Langmuir*, 2011, **27**, 11098–11105.

8. C.-C. Huang, P.-H. Lin and C.-W. Lee, *RSC Adv.*, 2016, **6**, 64494–64498.